

Label-free detection of proteins in ternary mixtures using surface-enhanced Raman scattering and protein melting profiles

Sercan Keskin
Esen Efeoğlu
Kaan Keçeci
Mustafa Çulha

Label-free detection of proteins in ternary mixtures using surface-enhanced Raman scattering and protein melting profiles

Sercan Keskin, Esen Efeoğlu, Kaan Keçeci, and Mustafa Çulha

Yeditepe University, Department of Genetics and Bioengineering, Atasehir, Istanbul 34755, Turkey

Abstract. The multiplex detection of biologically important molecules such as proteins in complex mixtures has critical importance not only in disease diagnosis but also in other fields such as proteomics and biotechnology. Surface-enhanced Raman scattering (SERS) is a powerful technique for multiplex identification of molecular components in a mixture. We combined the multiplexing power of SERS and heat denaturation of proteins to identify proteins in ternary protein mixtures. The heat denaturation profiles of four model blood proteins, transferrin, human serum albumin, fibrinogen, and hemoglobin, were studied with SERS. Then, two ternary mixtures of these four proteins were used to test the feasibility of the approach. It was demonstrated that unique denaturation profiles of each protein could be used for their identification in the mixture. © 2013 Society of Photo-Optical Instrumentation Engineers (SPIE) [DOI: 10.1117/1.JBO.18.3.037007]

Keywords: surface-enhanced Raman scattering; protein; multiplex detection; heat denaturation.

Paper 12544PR received Aug. 20, 2012; revised manuscript received Feb. 3, 2013; accepted for publication Feb. 18, 2013; published online Mar. 20, 2013.

1 Introduction

As the end product of gene expression, proteins carry out numerous functions in living systems. Therefore, their detection and identification have critical importance in many fields such as medicine, biotechnology, and proteomics. The mass spectroscopy (MS) and immunoassay-based methods are the most frequently used approaches for the goal. The MS-based approaches are the most sensitive and reliable ones without any question. However, most of the time, it requires a separation step before the analysis, and high cost instrumentation and highly trained personal. In addition, the destructive nature of the technique could constrain its use with the samples in limited amounts.^{1,2} The immunoassay-based methods are more straightforward compared to MS-based approaches but they are prone to false readings and the quantification could be problematic.³

Surface-enhanced Raman scattering (SERS) is a nondestructive vibrational spectroscopic technique that can provide detailed information about the chemical structure of molecules or molecular structures with high sensitivity.^{4,5} There are a number of reports using the technique for the detection and identification of a wide range of biological molecules and structures such as protein,^{6–10} DNA, RNA, oligonucleotide,^{11–14} bacteria,^{15–17} yeast,¹⁸ viruses,^{19,20} and living cells^{21–23} in the literature. These reports demonstrate the feasibility and potential of the technique towards the goal.

Despite all the advantages of SERS, it still suffers from issues such reproducibility and substrate stability when especially colloidal noble metal nanoparticles are used as substrates. Besides, if a molecule of interest has a complex structure possessing similar repeating units with multiple functional groups such as a protein, the problems attributed to the nature of SERS

become more considerable.^{24,25} However, the reports to date demonstrated that one of the most suitable substrates for protein-SERS studies appears to be aggregates of Ag colloidal particles (AgNPs) synthesized with citrate reduction of Ag⁺. Since colloidal AgNPs provide outstanding SERS enhancement and its preparation procedure is simple and low cost, it is routinely used as SERS substrates.^{6–10,26}

In SERS studies of proteins, external Raman-active dyes can be used to obtain intense SERS signal, but the obtained SERS spectrum cannot provide any information about the protein structure. In addition, use of a label lengthens procedure and it may result with the nonspecific interaction of the label with substrates.^{27,28} Therefore, label-free approaches are considered more reliable. The label free-detection of proteins with SERS is an ongoing effort but it has certain difficulties due to their highly complex structures and surface properties. Therefore, it is a challenging task to develop a universally accepted SERS protocol for the label-free protein detection.^{6–10,24–26}

Generally, the sample preparation steps in a SERS experiment upon using colloidal metal nanoparticles follow the order of simple mixing of analyte with a small volume of colloidal suspension of the noble metal nanoparticles, spotting this mixture on a proper surface, and acquisition of SERS spectra from the aggregates of noble metal nanoparticles distributed in the droplet area after the evaporation of water. This procedure is quite simple, but the phenomenon known as “coffee-ring” governs the dynamic processes in a sessile droplet during drying and all particles and molecules in the droplet are dragged and jammed at the solid-liquid-air contact line.²⁹ This uncontrolled aggregation of AgNPs and proteins at the periphery of the droplet is not suitable for a successful SERS measurement due to the tight packing of AgNPs and proteins, which is not a condition for the optimal oscillation of electron systems of AgNPs. This

Address all correspondence to: Mustafa Çulha, Yeditepe University, Department of Genetics and Bioengineering, Atasehir, Istanbul 34755, Turkey. Tel: +90 (216) 5781587; Fax: +90 (216)5780829; E-mail: mculha@yeditepe.edu.tr

poor oscillation eventually leads to a decrease in the SERS activity.^{7–10} In order to eliminate the negative effects of the coffee-ring phenomenon on the SERS performance of the AgNP aggregates, we altered the dynamics in a droplet by hanging it from a relatively hydrophobic surface.⁷ The gravity force causes the accumulation of the AgNPs and proteins at the apex of the drying droplet and after the complete evaporation of the liquid, most of the AgNPs and proteins attach in the middle of the dried droplet area. These accumulated AgNP-protein structures in the middle of the droplet area were found more suitable for a successful SERS measurement than the structures at the edges of the droplet generated by the conventional method. The feasibility and details of the suspended droplet method were recently reported by Keskin et al.⁷

Most of the previous studies based on label-free protein detection employing SERS used samples that contained only one type of protein.^{7,26,30–33} As an exception, Keskin et al. achieved the differential separation of the binary and ternary protein mixtures with the method known as “convective assembly” and detection with SERS.⁸ In another previous report, Zhen et al. used a mixture of proteins, some contain chromophore and some do not, and performed protein detection in their binary mixtures with using a heat-induced SERS method.³⁴ In a recent study, our group investigated the conformational changes in the structure of the model proteins with SERS at increased temperatures to 70°C from 30°C for detection and identification in binary mixtures.⁹ We coupled the fingerprint property of SERS with unique denaturation profiles of proteins as a new approach for label-free protein detection and identification. The conformational changes in the structure of proteins at varying temperatures with using SERS were previously investigated by Das et al.³⁵ In their study, lysozyme, ribonuclease B, bovine serum albumin, and myoglobin were studied with a temperature gradient between –65°C and 90°C.

In this current study, we used colloidal AgNPs as substrates and the human plasma proteins; human serum albumin (HSA), transferrin (TF), hemoglobin (Hb), and fibrinogen as models. The proteins were simply mixed with colloidal suspension of AgNPs and dried at suspended position from a hydrophobic surface. We investigated the conformational changes in the structures of the proteins among AgNP aggregates in dried droplet area with SERS at a temperature gradient from 30°C to 70°C. We set the starting temperature to 30°C due to its closeness to the room temperature. The system is heated to a maximum of 70°C since the denaturation temperatures of all model proteins in the study are lower than 70°C, which was predicted in their aqueous solution with dynamic light scattering (DLS) technique. The denaturation profiles of the model proteins are found unique and significantly different from each other, which can be used for their detection in mixtures. Two different ternary mixture combinations, which are HSA–transferrin–Hb and HSA–fibrinogen–Hb, were investigated. A statistical program, SPSS (statistical package for the social sciences), was used to analyze the obtained SERS spectra.

2 Materials and Methods

2.1 Chemicals

Human serum albumin, transferrin, hemoglobin, and fibrinogen were purchased from Sigma-Aldrich (Germany). Silver nitrate was purchased from Fluka (Germany) and sodium citrate was

purchased from Merck (Germany). Ultra pure water was used for preparing protein stock solutions.

2.2 Synthesis of AgNP Colloidal Suspension

AgNPs were prepared by using the Lee and Meisel method.³⁶ A 90 mg of AgNO₃ was dissolved in 500 mL double distilled water and heated until boiling point. Then, a 10 mL of 1% sodium citrate was added dropwise into the solution and boiling was maintained until the volume of the solution was reduced to approximately 250 mL. This prepared solution was kept at room temperature for cooling. The characterization of the colloidal AgNPs was performed with UV/Vis Spectroscopy and Dynamic Light Scattering (DLS, Zetasizer). The average diameter of AgNPs is approximately 55 nm (data not shown). The concentration of the AgNP suspension is called 1× and the suspension was centrifuged (Beckman, Rotor: S4180) at 5500 rpm for 30 min. Then, the supernatant of the solution was removed to bring the final concentration to 8× and it was used for all the experiments in the study.

2.3 Sample Preparation

The protein solutions were prepared in the concentration of 100 µg/mL and they were mixed with 8× AgNP colloidal suspension to bring the final protein and AgNP concentration to 50 µg/mL and 4×, respectively. Each protein concentration in all mixtures in the study is 50 µg/mL. A volume of 2 µL protein and colloidal AgNP mixture was spotted on a CaF₂ slide (hydrophobic). Then, the CaF₂ slide was fixed to a clamp at the overturned position (with an angle of 180 deg around its own axis). The position of the clamp was maintained until the droplet completely dried at room temperature. The room temperature and relative humidity were 22°C to 25°C and 40% to 50%, respectively, during the experiments.

2.4 SERS Measurement

A Raman microscopy system (InVia Reflex, Renishaw, United Kingdom) was used to perform all SERS measurements in the study. The system was calibrated against a silicon wafer peak at 520 cm⁻¹. A diode laser at 830 nm was used. The laser power of 15 mW was used for all measurements. A long-range objective was used with the heating apparatus (THMS600) to prevent the objective from any damage caused by high temperature. The exposure time of laser on the sample is 10 s. The temperature of the heating system was increased gradually from 30°C to 70°C with 10°C intervals and five SERS spectra were collected at every point (at 30°C, 40°C, 50°C, 60°C, and 70°C) and averaged to one spectrum.

2.5 Size and Zeta Potential Measurement

The size distribution measurements of the proteins in 1% phosphate buffered saline (PBS) at a temperature gradient between 30°C and 80°C were performed using Zetasizer NanoZS (Malvern). Their zeta potential measurements were also performed at 25°C. The Nano ZS contains a 4 mW He-Ne laser operating at a wavelength of 633 nm and an avalanche photodiode detector. The scattered light was detected at an angle of 173 deg. The refractive index and absorption of the protein solutions were assumed as 1.45 and 0.001, respectively.

2.6 SPSS Analysis

The obtained SERS spectra were analyzed with using SPSS 15.0. After the normalization of the spectra, they were analyzed with the multidimensional scaling feature of SPSS. The Euclidean distances were used as a scaling model and two-dimensional (2-D) plots were used for the presentation of the data.

3 Results and Discussions

In this method, proteins and AgNPs are accumulated in the middle of a dried droplet area by the force of gravity. These easily prepared protein-AgNP aggregates are favorable to collect SERS spectrum and the quality and reproducibility of the obtained spectra are remarkably improved compared to other techniques.^{10,25,26,37-41}

In the first part of the study, we determined the melting temperatures of the model proteins in their suspensions with the DLS technique. We used these melting point values as a starting point to analyze and compare the SERS spectra of the proteins during heat denaturation. The physicochemical properties and approximate melting point values of the proteins were shown on Table 1. The melting point of fibrinogen could not be determined with DLS due to the linear structure of the fibrinogen molecule, which is not suitable so as to the limitation of technique. As seen on Table 1, HSA and transferrin have similar melting point values. On the other hand, hemoglobin, which has a heme group consisting of an iron (Fe) ion hold in a heterocyclic ring known as a porphyrin, has a lower melting point compared to other proteins used in the study.

In the second part of the study, we investigated the heat denaturation profiles of proteins with SERS in their dried aggregates. The changes on the SERS spectra are specific for each protein and can be used for the identification of the proteins. We used a statistical program, SPSS, to determine the similarities or differences between the spectra obtained at different temperatures. In multi-dimensional scaling of SPSS, each spectrum can be reduced into one point on a 2-D coordinate system using Euclidean distances. The most straightforward and generally accepted way of computing distances between objects in a multi-dimensional space is to compute Euclidean distances. The closeness of the coordinates indicates the close relationship among the spectra.

Figure 1(a) shows the SERS spectra of HSA at a temperature gradient with 10°C steps and Fig. 1(b) shows the 2-D Euclidean distances plot. The melting point of HSA was found 64°C in solution. As seen in Fig. 1(b), obtained spectra at different temperatures located on very different coordinates relative to each other on the 2-D plot and the spectra at 30°C differ most from the others. A careful inspection of the spectra at different temperatures reveals that the intensity of the several bands changes with the temperature change. When the spectra are compared, two spectra at 30°C and 70°C show the greatest difference compared to the others as seen on Fig. 1(b). The reason for this difference at 30°C is the intense peaks at the bands, 628 (COO⁻ wag.), 928 (Pro), 955 (Ala), and 1001 cm⁻¹ (Phe). Since this is just the beginning of the temperature gradient, denaturation of the proteins is not expected. This is possibly due to better oscillation of the electron system of the AgNPs with the loss of water molecules from the sample, which has a considerable effect on the excitation of surface plasmons. The spectra at 40°C, 50°C,

Table 1 Physicochemical properties and approximate melting point values of proteins.

Protein	MW (kDa)	Hydrodynamic radius (nm)	Isoelectric point (pI)	Zeta potential (mV)	Melting point (°C)
HSA	66.5	7.937	4.7–5.2	–28.9	64
Transferrin	76 to 81	15.55	5,5	–18.4	68
Fibrinogen	340	15.68	5.8–6.1	–9.53	–
Hemoglobin	64.5	8.911	6.8	13	42

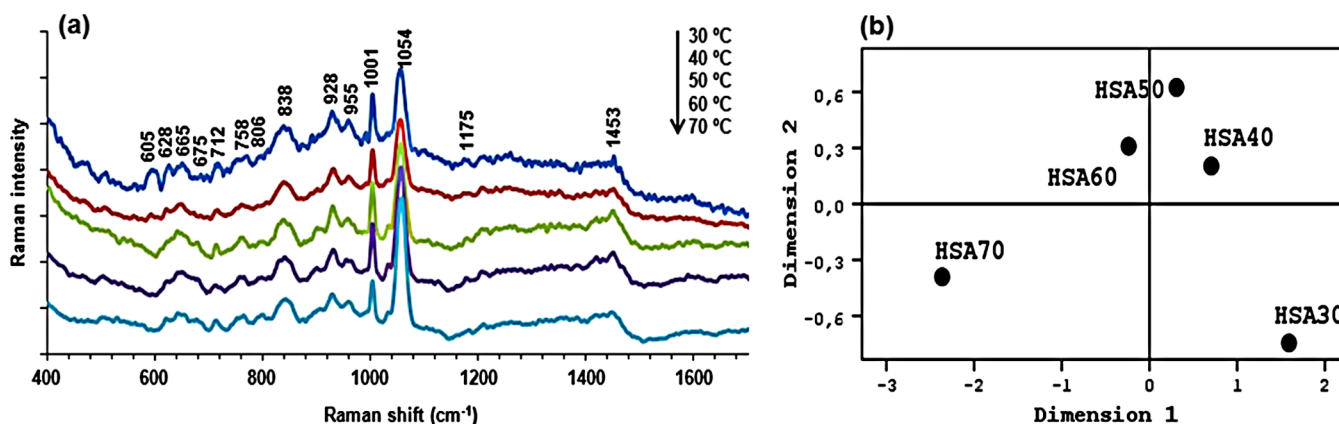


Fig. 1 (a) SERS spectra of HSA at increased temperatures and (b) 2-D Euclidean distances plot. The numbers on the plot (b) represent the temperature values.

and 60°C are very stable and similar to each other compared to the spectra at 30°C. When the temperature reaches 70°C, which is around the melting point of HSA, the spectra are located on different coordinates due to the significant decreasing in the intensities of the bands at 928, 955, and 1001 cm⁻¹. This suggests that the environment of these residues change at 70°C as a result of the conformational changes of HSA molecules in the AgNP-protein structures. The assignments of all the Raman bands in the study are given in Table 2 in Appendix B.⁴²⁻⁵⁰

Figure 2(a) shows the SERS spectra of transferrin with temperature gradient and Fig. 2(b) shows the 2-D Euclidean distances plot. As seen in Fig. 2(a), a significant change is observed in the region from 620 to 680 cm⁻¹. The melting temperature of transferrin was found at approximately 68°C in solution. On the 2-D plot, the spectra at 60°C and 70°C placed relatively far from other spots on the plot with relative closeness to each other. This suggests that the structure of transferrin shows a noteworthy change at some point between 60°C and 70°C.

The intensities of the peaks at 676 and 1001 cm⁻¹, which are both associated with Phe, gradually increase from 30°C to 60°C. For example, human serum transferrin has two domains and contains 28 Phe residues.⁵¹ The increase in the intensity of the

these two bands can be explained with the gradual denaturation of the protein with increasing temperature. As the denaturation of protein progresses, Phe residues interact with the AgNPs more effectively, which is reflected on the SERS spectra as an increase in the intensity of the peaks attributed to Phe at 676 and 1001 cm⁻¹. The intense peak at around 1053 cm⁻¹, which is observed in the SERS spectra of all the proteins in the study, is attributed to C—O str. It may originate from both citrate ions^{7,26} and protein structures.⁴³ The citrate ions are adsorbed onto the NPs' surfaces during their synthesis. The intense peak at around 1053 cm⁻¹ is the only significant feature of the SERS spectra of the sample that contains only AgNPs (Fig. 7 in Appendix A).

Figure 3(a) shows the SERS spectra of Hb with temperature gradient and Fig. 3(b) shows the 2-D Euclidean distances plot. The melting point of Hb was found 42°C in solution, which is lower than the melting points of other proteins used in the study. Therefore, it can be a suitable model protein for investigating the potential of the approach. Since it has a lower melting temperature than the other proteins, the structural changes will be easier to distinguish in the mixture. As seen in Fig. 3(a), the intensity of the peak at 937 cm⁻¹, which is associated with Pro, decreases

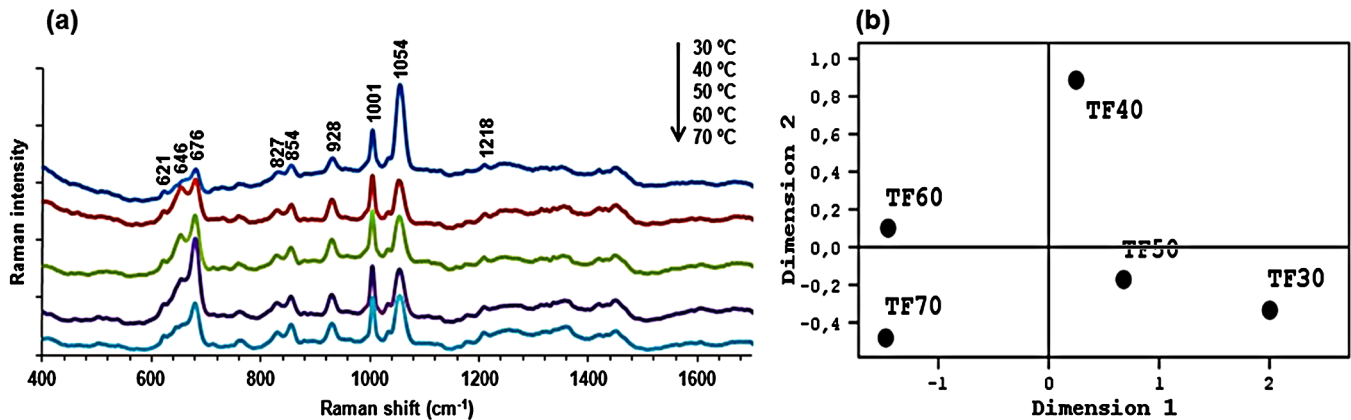


Fig. 2 (a) SERS spectra of transferrin at increasing temperatures and (b) 2-D Euclidean distances plot. The numbers on the plot (b) represent the temperature values.

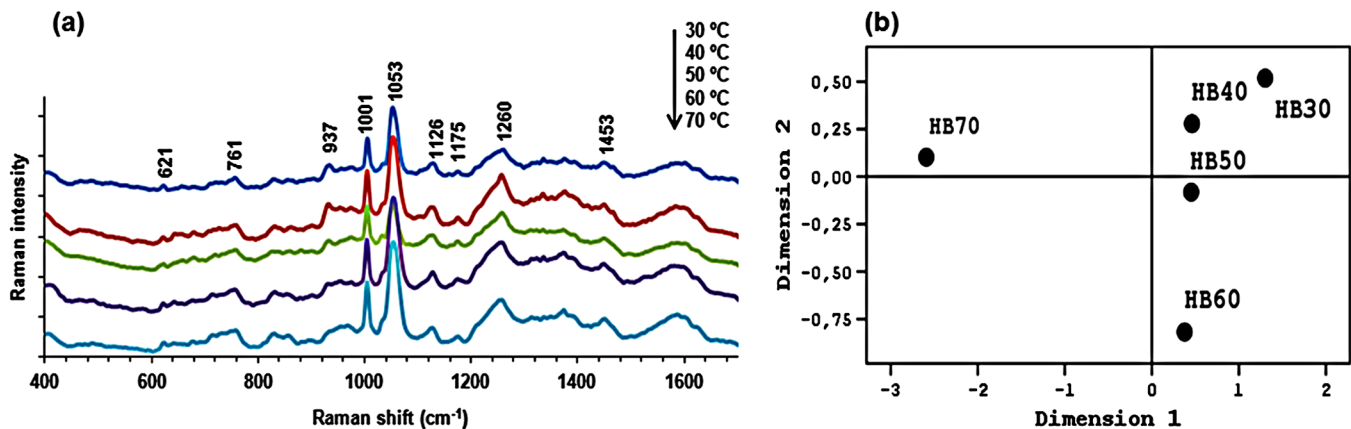


Fig. 3 (a) SERS spectra of hemoglobin at increasing temperatures and (b) 2-D Euclidean distances plot. The numbers on the plot (b) represent the temperature values.

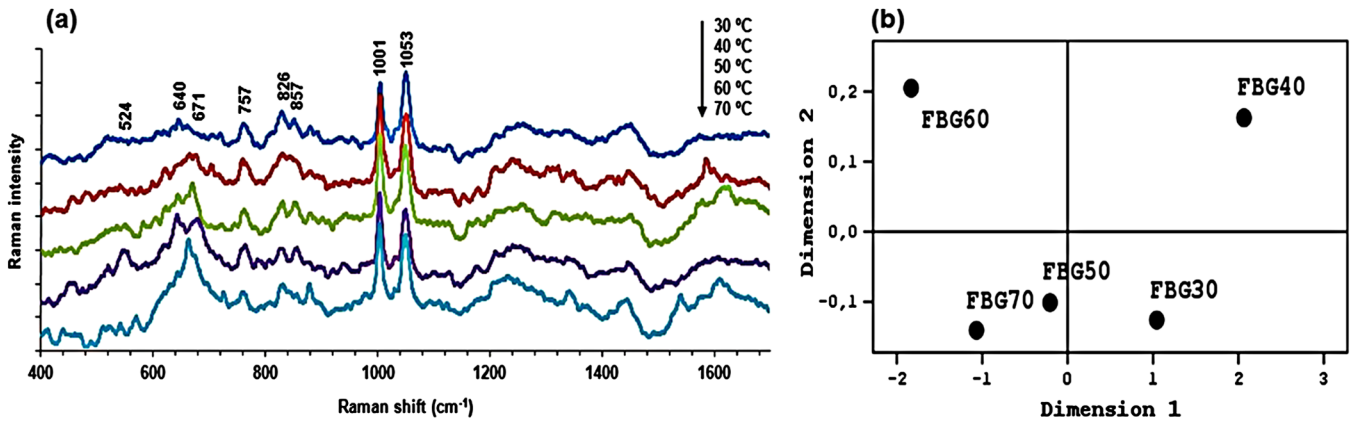


Fig. 4 (a) SERS spectra of fibrinogen at increased temperatures and (b) 2-D Euclidean distances plot. The numbers on the plot (b) represent the temperature values.

while the temperature increases and it completely disappears at 70°C. Additionally, the intensity of the peak at 1260 cm⁻¹, which is attributed to Amide III vibration, shows a significant increase at 40°C, compared to the intensity of the peak at 30°C. Note that 40°C is close to the melting point of Hb. In Fig. 3(b), a significant difference among the spectra recorded at increasing

temperature is observed at 70°C. Although the temperatures at 50°C and 60°C are closer to the melting temperature of Hb in solution, the greater difference is observed at 70°C. This difference can be explained with a behavioral difference of protein in solution and in the dried film. In water, they can behave more freely, which leads to a more effective and fast response

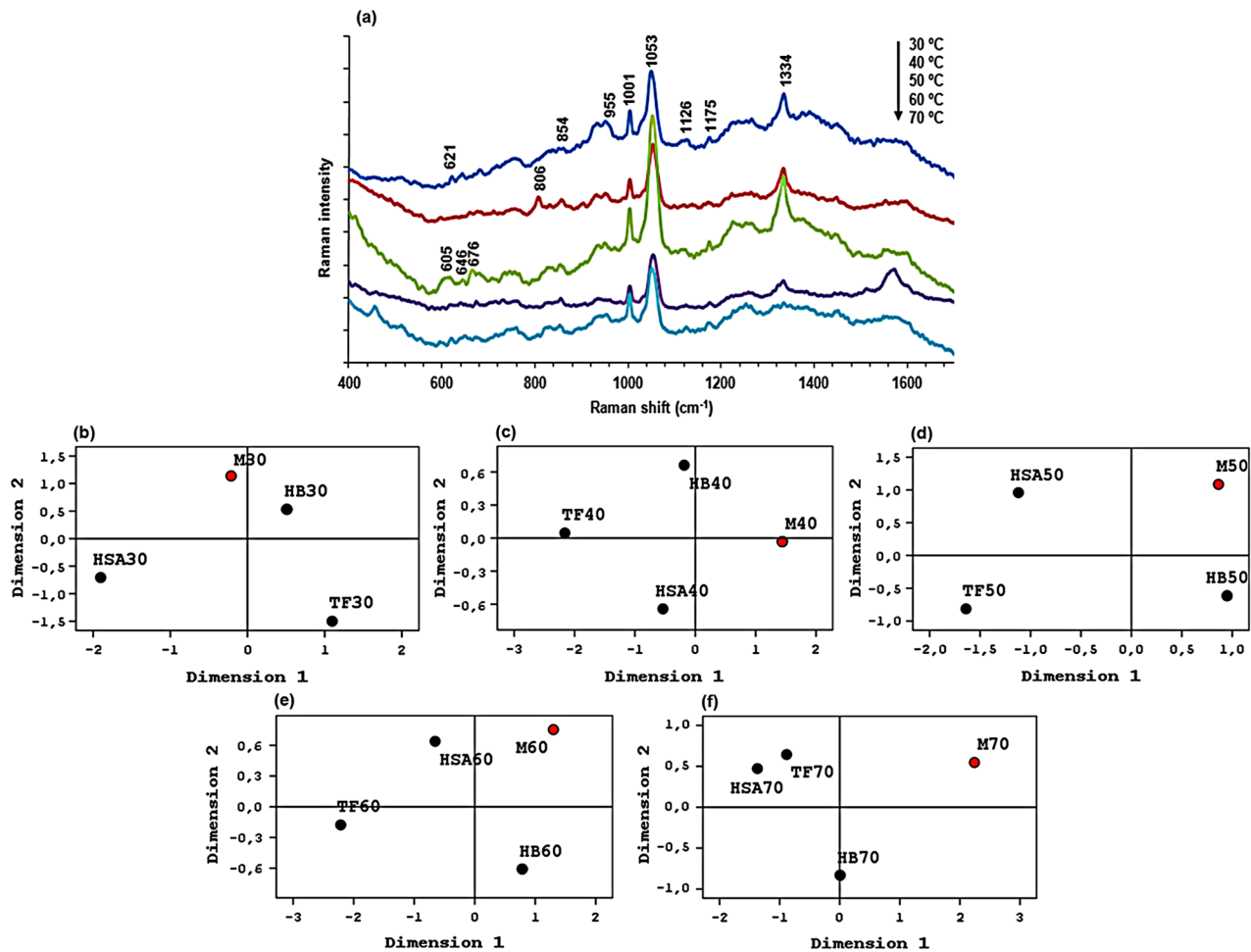


Fig. 5 (a) SERS spectra of HSA, transferrin and Hb mixture at increased temperatures and 2-D Euclidean distances plots for each temperature [(b) 30°C, (c) 40°C, (d) 50°C, (e) 60°C, and (f) 70°C]. HB: hemoglobin; TF: transferrin; and M (red): mixture. The numbers on the plots (b) to (f) represent the temperature values.

to changes in temperature. In SERS measurement, we used dried samples that also contain AgNPs. Therefore, it requires more time and higher temperature for proteins to respond to the temperature increase.

The last model protein included in the study was fibrinogen, which is another blood plasma protein and plays a crucial role in hemostasis. Even though the melting point of fibrinogen could not be determined in solution with DLS, there are a number of reports demonstrated that fibrinogen is very sensitive to heat and its structure shows dramatic changes between 60°C and 70°C.^{52,53} Figure 4(a) shows the SERS spectra of fibrinogen with temperature gradient and Fig. 4(b) shows the 2-D Euclidean distances plot. We have also observed a significant change on the SERS spectra of fibrinogen at 60°C and 70°C, which can be seen in Fig. 4(a). The intense peak at 640 cm⁻¹, which is obtained at 60°C, is associated with Tyr residues. Also, another intense peak at 671 cm⁻¹, which is observed at 70°C, is associated with C–C stretching. The broad peak at around 524 cm⁻¹ is associated with S–S disulfide stretching. The peak at 757 cm⁻¹ is associated with Trp and the peaks

at 826 and 857 cm⁻¹ are associated with Pro and Ala, respectively. As seen in Fig. 4(b), the spectra at 60°C show a significant difference from the other spectra. There is also another significant difference between the spectra obtained at 60°C and 70°C. This indicates that the structure of fibrinogen changes starting from 50°C and the temperature values of 60°C and 70°C are critical points in this differentiation.

Finally, we attempted to identify each protein in their ternary mixtures using the proposed approach. In the first model ternary mixture, we used HSA, transferrin, and Hb to mix with the colloidal suspension of the AgNPs and spotted a 2 μL volume of this mixture on a CaF₂ surface. After the sample completely dried at suspended configuration at room temperature, we collected SERS spectra at increasing temperatures. The proteins in the mixture have different melting points. Therefore, it is expected that the structure of each protein starts to change at a different point of the temperature scale. This change can be observed on the SERS spectra. Figure 5(a) shows the SERS spectra of HSA, transferrin, and Hb mixture at increased

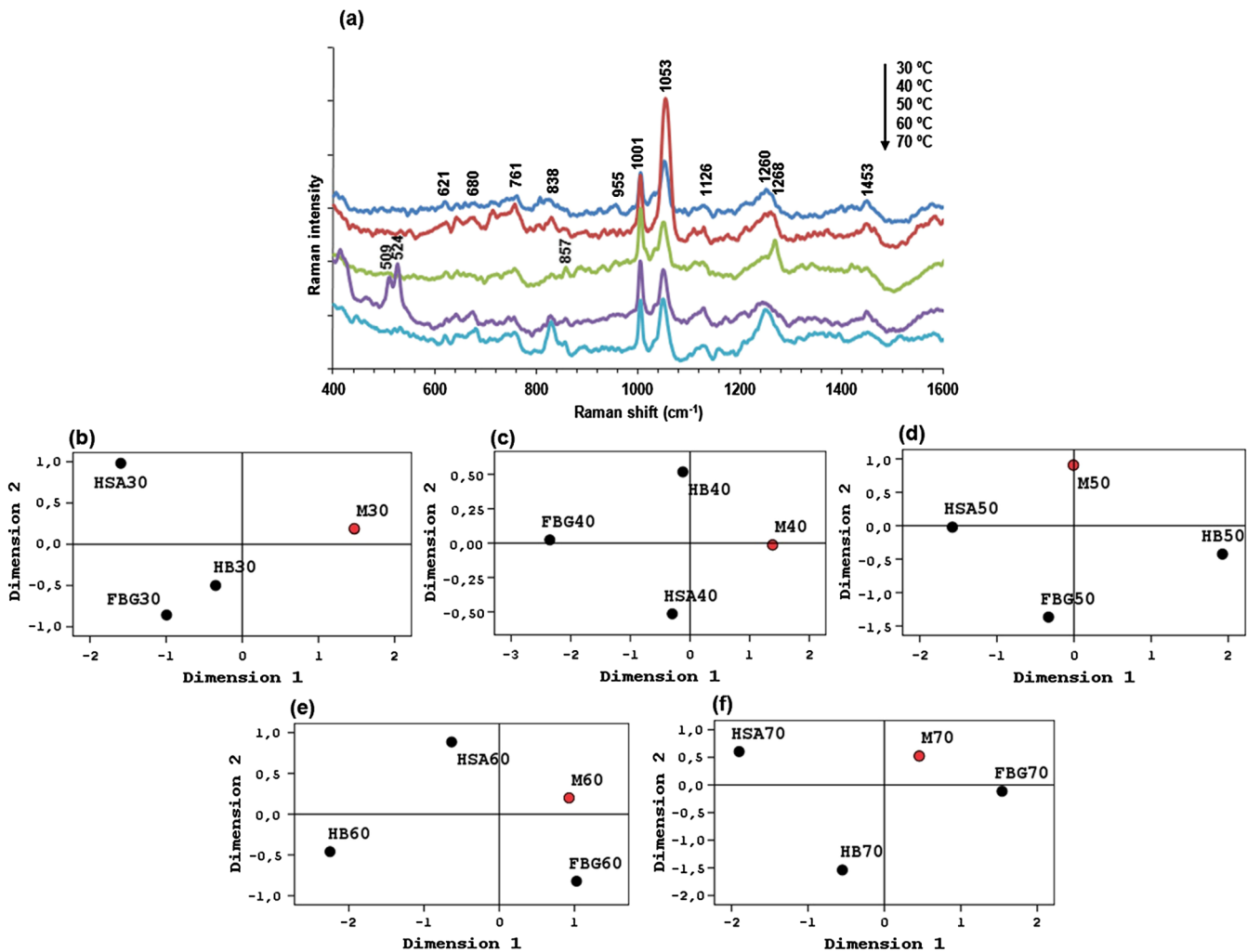


Fig. 6 (a) SERS spectra of HSA, fibrinogen and hemoglobin mixture at increasing temperatures and 2-D Euclidean distances plots for each temperature [(b) 30°C, (c) 40°C, (d) 50°C, (e) 60°C, and (f) 70°C]. HB: hemoglobin; FBG: fibrinogen; and M (red): mixture. The numbers on the plots (b) to (f) represent the temperature values.

temperatures and 2-D Euclidean distances plots for each temperature [Fig. 5(b) 30°C, 5(c) 40°C, 5(d) 50°C, 5(e) 60°C, and 5(f) 70°C]. The concentration of each protein and AgNPs are 50 $\mu\text{g}/\text{mL}$ and 4 \times , respectively. As seen in Fig. 5(a), the SERS spectra of the mixture have more spectral features than the individual spectra of the proteins due to the interaction of different proteins with AgNPs and also each other. The intense peak at 1334 cm^{-1} , which is associated with Trp, is a result of this protein-protein interaction, since it could not be observed on the individual SERS spectra of the proteins. The peak at 854 cm^{-1} , which is associated with Ala residues, belongs to transferrin since it can also be observed on the spectra of the sample that contains only transferrin [Fig. 2(a)]. The peak at 1126 cm^{-1} , which is associated with NH_3^+ deformation of Leu, belongs to Hb. As seen in Fig. 4(b)–4(d), the spectra of the mixture are close to the spectra of the Hb at 30°C, 40°C, and 50°C. Note that these temperature values are close to the melting point of Hb, which was found as 42°C. The broad peak at 605 cm^{-1} is observed at 50°C. Note that the peak at 605 cm^{-1} is also observed in the SERS spectra of the sample that contain only HSA [Fig. 1(a)]. When the temperature reaches 60°C, the spectra of the mixture show more resemblance to the spectra of HSA [Fig. 5(e)]. It should be noted that 60°C is close to the melting point of HSA, which was found to be 64°C. In summary, the spectra of the mixture have a different pattern from the individual spectra of each protein and also have unexpected spectral features due to the intermolecular interactions among proteins (before and after denaturation) in the mixture. Therefore, it is difficult to observe small differences in the SERS spectra for comparison. However, the 2-D plots indicate that when a protein reaches its melting point, it starts to dominate the spectra of the mixture. The structure of Hb denatures in the range of 30°C to 40°C and the surfaces of AgNPs are exposed to the amino acid residues of Hb effectively. When the temperature reaches to the range of 50 to 60°C, the same case was observed for HSA and when it is 70°C, transferrin molecules show their impact more effectively.

Figure 6(a) shows the SERS spectra of the second set of protein mixture composed of HSA, fibrinogen, and Hb at increased temperatures and 2-D Euclidean distances plots for each temperature [Fig. 6(b) 30°C, 6(c) 40°C, 6(d) 50°C, 6(e) 60°C, and 6(f) 70°C]. The concentration of each protein and AgNPs are 50 $\mu\text{g}/\text{mL}$ and 4 \times , respectively. As seen in Fig. 6(a), the bands at 1126 and 1260 cm^{-1} are associated with Hb and the intensity of the peak at 1260 cm^{-1} is increasing when the temperature reaches around 40°C. This point is also close to the melting point of Hb and as seen in Fig. 6(c), the spectra of Hb are approaching the spectra of the mixture at 40°C. When the temperature reaches to 60°C, the spectra of the mixture become similar to the spectra of HSA and fibrinogen and show a significant difference from the spectra of Hb. Note that the melting points of both HSA and fibrinogen are between 60°C and 70°C. The intensity of the peak at 838 cm^{-1} , which arises from HSA, starts to increase at 60°C. Therefore, the spectra of the mixture are close to the spectra of HSA at 60°C. When the temperature reaches 70°C, the spectra of the mixture show more resemblance to the spectra of Hb again (compared to the spectra at 60°C) due to the intense peak at 1260 cm^{-1} , which arises from Hb. This peak at 1260 cm^{-1} (CH_2 wag.) is associated with both heme group and backbone of Hb molecule. The spectra of the mixture

also resemble to the spectra of fibrinogen at 60°C and 70°C [Fig. 6(e) and 6(f)] due to the intense peak at 524 cm^{-1} , which could also be observed on the individual spectra of fibrinogen. Therefore, we can suggest that the changes occurring in the structure of proteins could be observed not only on their individual SERS spectra but also in the spectra of their ternary mixtures.

4 Conclusion

In this study, we demonstrated the feasibility of a combined approach of temperature gradient and SERS for protein identification in their mixtures. The colloidal AgNPs and HSA, transferrin, Hb, and fibrinogen as substrates and model proteins are used, respectively. As the temperature increases, protein molecules start to denature and this is reflected to the SERS spectra. The melting temperature of each protein in their solution was used to relate the changes in SERS spectra of the proteins. The obtained information from their SERS spectra during temperature gradient was used for their identification in ternary mixtures. The results indicate that proteins can show different behaviors in multiple mixtures due to their interaction with each other and the AgNPs, which further complicates the interpretation of the SERS spectra. However, from the analysis of the data, it can be suggested that when a protein in a multiple mixture reaches its melting (denaturation) point, it causes an observable impact on the SERS spectra of the mixture and this can be used for the routine detection of proteins in mixtures composed of proteins. We continue to investigate influence of protein concentration on the spectral changes during the temperature gradient. Successful implementation of such a technique can serve the detection and identification of proteins obtained from a known source such as blood after a crude separation step.

Appendix A

In this appendix, SERS spectrum of citrate-reduced AgNPs is presented for possible interferences (Fig. 7). An average of ten SERS spectra were acquired from different spots on the dried sample. As seen, the only significant feature of the spectrum is the intense peak at 1053 cm^{-1} , which is associated with C–O vibration of citrate ions adsorbed on NPs' surfaces.

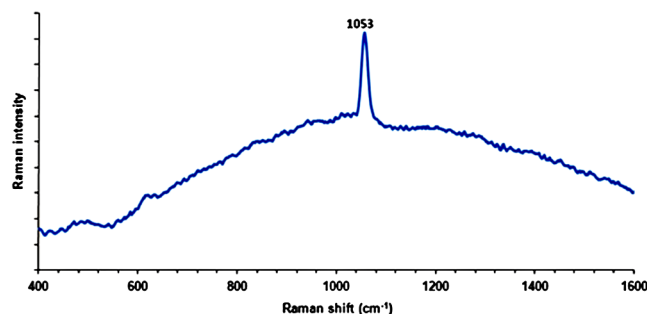


Fig. 7 SERS spectrum obtained from citrate-reduced AgNPs. The concentration of AgNP suspension was 4 \times in the dried sample.

Table 2 Band assignments of the SERS spectra of proteins and protein mixtures used in the study.

HSA	Transferrin	Hemoglobin	Fibrinogen	Mixture 1 ^a	Mixture 2 ^b	Band assignments
—	—	—	524	—	509, 524	S—S str. ^{42–44}
605	—	—	—	605	—	—
—	621	621	—	621	621	Phe ^{44,45}
628	—	—	—	—	—	COO ⁻ wag. ⁴⁶
—	—	—	640	—	—	Tyr ⁴³
—	646	—	—	646	—	Tyr ⁴⁷
665	—	—	—	—	—	—
—	—	—	671	—	—	C—C str. ⁴⁶
675	676	—	—	676	—	Ala ⁴⁶
—	—	—	—	—	680	—
712	—	—	—	—	—	Met ⁴²
758	—	761	757	—	761	Trp ⁴⁶
806	—	—	—	806	—	—
—	827	—	826	—	—	Pro, Tyr ⁴⁷
838	—	—	—	—	838	Vibration of amine groups ⁴⁸
—	854	—	857	854	857	Ala ⁴⁶
928	928	—	—	—	—	Pro, Val ⁴⁹
—	—	937	—	—	—	Pro ⁴⁴
955	—	—	—	955	955	Ala ⁴⁶
1001	1001	1001	1001	1001	1001	Phe ⁴⁶
1054	1054	1053	1053	1053	1053	C—O, C—N str. ⁴³
—	—	1126	—	1126	1126	C—N str. ⁵⁰
1175	—	1175	—	1175	—	Tyr ⁵⁰
—	1218	—	—	—	—	Amide III ⁴⁶
—	—	1260	—	—	1260, 1268	CH ₂ wag. ⁴⁶
—	—	—	—	1334	—	Trp ⁴⁶
1453	—	1453	—	—	1453	Gly ⁴⁶

^aHSA + transferrin + hemoglobin^bHSA + hemoglobin + fibrinogen

Appendix B

This appendix provides the assignments of the band frequencies, which are obtained from the SERS spectra of the proteins and protein mixtures (Table 2).

Acknowledgments

The authors acknowledge the financial support of the Scientific and Technological Council of Turkey (Project no: 109T941) and Yeditepe University.

References

1. J. Li et al., "Proteomics and bioinformatics approaches for identification of serum biomarkers to detect breast cancer," *Clin. Chem.* **48**(8), 1296–1304 (2002).
2. K. A. Baggerly, J. S. Morris, and K. R. Coombes, "Reproducibility of SELDI-TOF protein patterns in serum: comparing datasets from different experiments," *Bioinformatics* **20**(5), 777–785 (2004).
3. G. P. Murphy et al., "Current evaluation of the tissue localization and diagnostic utility of prostate-specific membrane antigen," *Cancer* **83**(11), 2259–2269 (1998).

4. M. Moskovits, "Surface-enhanced spectroscopy," *Rev. Mod. Phys.* **57**(3), 783–826 (1985).
5. S. Lee et al., "Biological imaging of HEK293 cells expressing PLCgamma1 using surface-enhanced Raman microscopy," *Anal. Chem.* **79**(3), 916–922 (2007).
6. M. Wang et al., "Optofluidic device for ultra-sensitive detection of proteins using surface-enhanced Raman spectroscopy," *Microfluid. Nanofluid.* **6**(3), 411–417 (2009).
7. S. Keskin and M. Culha, "Label-free detection of proteins from dried-suspended droplets using surface enhanced Raman scattering," *Analyst* **137**(11), 265–2657 (2012).
8. S. Keskin, M. Kahraman, and M. Culha, "Differential separation of protein mixtures using convective assembly and label-free detection with surface enhanced Raman scattering," *Chem. Commun.* **47**(12), 3424–3426 (2011).
9. M. Culha and S. Keskin, "Surface-enhanced Raman scattering for label-free protein detection and identification," *Proc. SPIE* **8234**, 823407 (2012).
10. M. Culha et al., "Manipulation of silver nanoparticles in a droplet for label-free detection of biological molecules using surface-enhanced Raman scattering," *Proc. SPIE* **7911**, 791102 (2011).
11. S. E. J. Bell and N. M. S. Sirimuthu, "Surface-enhanced Raman spectroscopy (SERS) for sub-micromolar detection of DNA/RNA mononucleotides," *J. Am. Chem. Soc.* **128**(49), 15580–15581 (2006).
12. W. Yuan et al., "Surface-enhanced Raman scattering biosensor for DNA detection on nanoparticle island substrates," *Appl. Opt.* **48**(22), 4329–4337 (2009).
13. M. Culha et al., "Surface-enhanced Raman scattering (SERS) substrate based on self-assembled monolayer (SAM) for use in gene diagnostics," *Anal. Chem.* **75**(22), 6196–6201 (2003).
14. Y. C. Cao, R. Jin, and C. A. Mirkin, "Nanoparticles with Raman spectroscopic fingerprints for DNA and RNA detection," *Science* **297**(5586), 1536–1540 (2002).
15. M. Kahraman et al., "Characterization of yeast using surface-enhanced Raman scattering," *Appl. Spectros.* **63**(11), 1276–1282 (2009).
16. M. Culha et al., "Characterization of thermophilic bacteria using surface-enhanced Raman scattering," *Appl. Spectros.* **62**(11), 1226–1232 (2008).
17. M. Kahraman et al., "Convective-assembly of bacteria for surface-enhanced Raman scattering," *Langmuir* **24**(3), 894–901 (2008).
18. I. Sayin et al., "Characterization of yeast using surface-enhanced Raman scattering," *Appl. Spectros.* **63**(11), 1276–1282 (2009).
19. S. Shanmukh et al., "Rapid and sensitive detection of respiratory virus molecular signatures using a silver nanorod array SERS substrate," *Nano Lett.* **6**(11), 2630–2636 (2006).
20. T. A. Alexander, "Development of methodology based on commercialized SERS-active substrates for rapid discrimination of Poxviridae virions," *Anal. Chem.* **80**(8), 2817–2825 (2008).
21. J. Kneipp et al., "Novel optical nanosensors for probing and imaging live cells," *Nanomed. Nanotechnol. Biol. Med.* **6**(2), 214–226 (2010).
22. H. W. Tang et al., "Chemical probing of single cancer cells with gold nanoaggregates by surface-enhanced Raman scattering," *Appl. Spectros.* **62**(10), 1060–1069 (2008).
23. K. Kneipp et al., "Surface-enhanced Raman spectroscopy in single living cells using gold nanoparticles," *Appl. Spectros.* **56**(2), 150–154 (2002).
24. X. X. Han, B. Zhao, and Y. Ozaki, "Surface-enhanced Raman scattering for protein detection," *Anal. Bioanal. Chem.* **394**(7), 1719–1727 (2009).
25. Z. Zhou et al., "Experimental parameters for the SERS of nitrate ion for label-free semi-quantitative detection of proteins and mechanism for proteins to form SERS hot sites: a SERS study," *J. Raman Spectros.* **42**(9), 1713–1721 (2011).
26. M. Kahraman, I. Sur, and M. Culha, "Label free detection of proteins from self-assembled protein-silver nanoparticle structures using surface enhanced Raman scattering," *Anal. Chem.* **82**(18), 7596–7602 (2010).
27. Y. C. Cao et al., "Raman dye-labeled nanoparticle probes for proteins," *J. Am. Chem. Soc.* **125**(48), 14676–14677 (2003).
28. D. S. Grubisha et al., "Femtomolar detection of prostate-specific antigen: an immunoassay based on surface-enhanced Raman scattering and immunogold labels," *Anal. Chem.* **75**(21), 5936–5943 (2003).
29. R. D. Deegan et al., "Capillary flow as the cause of ring stains from dried liquid drops," *Nature* **389**(6653), 827–829 (1997).
30. D. Zhang et al., "Raman detection of proteomic analytes," *Anal. Chem.* **75**(21), 5703–5709 (2003).
31. C. D. Keating et al., "Protein: colloid conjugates for surface enhanced Raman scattering: stability and control of protein orientation," *J. Phys. Chem. B* **102**(47), 9404–9413 (1998).
32. X. X. Han et al., "Highly sensitive protein concentration assay over a wide range via surface-enhanced Raman scattering of coomassie brilliant blue," *Anal. Chem.* **82**(11), 4325–4328 (2010).
33. F. Lu et al., "Protein-decorated reduced oxide graphene composite and its application to SERS," *ACS Appl. Mater. Interfaces* **4**(6), 3278–3284 (2012).
34. Z. Zhou et al., "Label-free detection of binary mixtures of proteins using surface-enhanced Raman scattering," *J. Raman Spectros.* **43**(6), 706–711 (2012).
35. G. Das et al., "Nano-patterned SERS substrate: application for protein analysis vs. temperature," *Biosens. Bioelectron.* **24**(6), 1693–1699 (2009).
36. P. C. Lee and D. Meisel, "Adsorption and surface-enhanced Raman of dyes on silver and gold sols," *J. Phys. Chem.* **86**(17), 3391–3395 (1982).
37. J. Baniukevic et al., "Magnetic gold nanoparticles in SERS-based sandwich immunoassay for antigen detection by well oriented antibodies," *Biosens. Bioelectron.* **43**(1), 281–288 (2013).
38. Y. Xia et al., "Aptasensor based on triplex switch for SERS detection of cytochrome c," *Analyst* **137**(24), 5705–5709 (2012).
39. O. Dong and D. C. C. Lam, "Silver nanoparticles as surface-enhanced Raman substrate for quantitative identification of label-free proteins," *Mater. Chem. Phys.* **126**(1–2), 91–96 (2011).
40. L. Chen et al., "Detection of proteins on silica-silver core-shell substrates by surface-enhanced Raman spectroscopy," *J. Colloid Interface Sci.* **360**(2), 482–487 (2011).
41. X. X. Han et al., "Analytical technique for label-free multi-protein detection based on Western blot and surface-enhanced Raman scattering," *Anal. Chem.* **80**(8), 2799–2804 (2008).
42. G. Shetty et al., "Raman spectroscopy: Elucidation of biochemical changes in carcinogenesis of oesophagus," *Br. J. Cancer* **94**(10), 1460–1464 (2006).
43. J. W. Chan et al., "Micro-Raman spectroscopy detects individual neoplastic and normal hematopoietic cells," *Biophys. J.* **90**(2), 648–656 (2006).
44. N. Stone et al., "Near-infrared Raman spectroscopy for the classification of epithelial pre-cancer and cancers," *J. Raman Spectros.* **33**(7), 564–573 (2002).
45. N. Stone et al., "Raman spectroscopy for identification of epithelial cancers," *Faraday Discuss.* **126**, 141–157 (2004).
46. S. Stewart and P. M. Frederics, "Surface-enhanced Raman spectroscopy of peptides and proteins absorbed on an electrochemically prepared silver surface," *Spectrochim. Acta Part A* **55**(7), 1615–1640 (1999).
47. W. T. Cheng et al., "Micro-Raman spectroscopy used to identify and grade human skin pilomatrixoma," *Microsc. Res. Tech.* **68**(2), 75–79 (2005).
48. D. Naumann, "Infrared and NIR Raman spectroscopy in medical microbiology," *Proc. SPIE* **3257**, 245–257 (1998).
49. D. P. Lau et al., "Raman spectroscopy for optical diagnosis in normal and cancerous tissue of the nasopharynx—preliminary findings," *Laser. Surg. Med.* **32**(3), 210–214 (2003).
50. I. Notingher et al., "Discrimination between ricin and sulphur mustard toxicity *in vitro* using Raman spectroscopy," *J. R. Soc. Interface* **1**(1), 79–90 (2004).
51. R. T. A. Macgillivray et al., "The complete amino acid sequence of human serum transferrin," *Proc. Natl. Acad. Sci. U. S. A.* **79**(81), 2504–2508 (1982).
52. S. Y. Lin et al., "Mechanical compression affecting the thermal-induced conformational stability and denaturation temperature of human fibrinogen," *Int. J. Biol. Macromol.* **37**(3), 127–133 (2005).
53. P. Schaaf et al., "Thermal denaturation of an adsorbed fibrinogen layer studied by reflectometry," *Langmuir* **3**(6), 1128–1131 (1987).